Crystal Structure of Phosphate Binding Protein Labeled with a Coumarin Fluorophore, a Probe for Inorganic Phosphate[†,‡]

Miriam Hirshberg,[*,§] Kim Henrick,[§,||] Lesley Lloyd Haire,[§] Nishi Vasisht,[§] Martin Brune,[⊥] John E. T. Corrie,[⊥] and Martin R. Webb[⊥]

Division of Protein Structure, National Institute for Medical Research, Mill Hill, London NW7 1AA, U.K., and Division of Physical Biochemistry, National Institute for Medical Research, Mill Hill, London NW7 1AA, U.K.

Received February 23, 1998; Revised Manuscript Received May 12, 1998

ABSTRACT: Crystal structures are presented for the A197C mutant of *Escherichia coli* phosphate binding protein (PBP) and the same mutant labeled at Cys197 with *N*-[2-(1-maleimidyl)ethyl]-7-(diethylamino)-coumarin-3-carboxamide (MDCC). Both proteins are complexed with inorganic phosphate. The latter molecule, MDCC−PBP, exhibits a large increase in fluorescence on binding inorganic phosphate. The resulting high-fluorescence state of the coumarin and the ability of this coumarin to monitor the conformational changes associated with inorganic phosphate binding are interpreted in terms of the specific interactions of MDCC with the protein. The structure helps to explain why this particular label gives a high-fluorescence state on binding inorganic phosphate, while several other related labels do not, and hence aids our general understanding of environmentally sensitive fluorescence probes on proteins.

In Gram-negative bacteria, binding proteins located in the periplasm are vital components of the active transport system of a large variety of essential molecules, including carbohydrates, amino acids, and inorganic ions. Inorganic phosphate (P_i) is bound by the phosphate binding protein (PBP),[1] which is a member of this class of proteins. PBP is produced under conditions of low P_i concentration, binds P_i in the periplasm, and transfers it to a membrane protein that transports it into the cytoplasm. Upon binding P_i, PBP undergoes a large conformational change (*1*), which seems to be a common feature of proteins belonging to the binding protein family (*2*).

The ability to monitor rapid changes of P_i concentration in real time contributes to our understanding of biological processes such as systems involving ATP and GTP hydrolysis. For this purpose, the A197C mutant of *Escherichia coli* PBP, labeled with a coumarin fluorophore [*N*-[2-(1-maleimidyl)ethyl]-7-(diethylamino)coumarin-3-carboxamide, MDCC] at Cys197, was developed as a fluorescent probe (MDCC−PBP) (*3*). Note that the maleimide moiety of MDCC becomes a succinimide as a consequence of its reaction with a thiol (Figure 1). The label at position 197 is on the edge of the P_i binding site, close enough to monitor the conformational changes associated with P_i binding without blocking the binding site itself. The observed increase in fluorescence intensity of MDCC−PBP upon binding P_i (*3*, *4*) presumably reflects the changes in the immediate environment of the coumarin as a consequence of the overall repositioning of the two domains of PBP. Its rapid response and high sensitivity have enabled this probe to be used in a number of different systems to measure P_i release kinetics in real time (*3*, *5*−*8*)

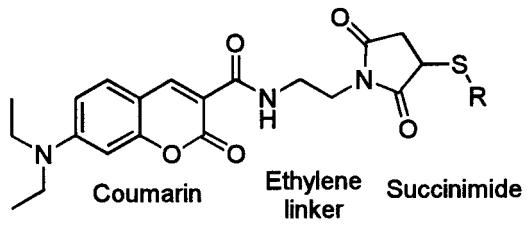

FIGURE 1: Structure of the MDCC−thiol adduct.

The development of this probe has led us to investigate in detail the mechanism of P_i binding to PBP. In the preceding paper (*4*), kinetic and spectroscopic measurements were used to study the P_i binding and to characterize the resultant high-fluorescence state. In this paper, we describe the crystal structures of both the unlabeled A197C PBP·P_i and MDCC−PBP·P_i and consider the structural features that may cause the high-fluorescence state of the coumarin.

The high-resolution structures of native PBP·P_i and the T141D mutant in both P_i-bound and P_i-free forms have been reported (*1*, *9*). Comparison between these structures and the ones presented here allowed analysis of the effects of both the single mutation (A197C) and the labeling on PBP structure. Moreover, using the structure of P_i-free T141D

† This work was funded by the Medical Research Council, U.K.

‡ The coordinates of the following structures have been deposited in the Brookhaven Protein Data Bank: A197C PBP·P_i (entry 1a54) and MDCC−PBP·P_i (entry 1a55).

* To whom correspondence should be addressed. Telephone: (44) 181 3666, ext 2520. Fax: (44) 181 906 4477. E-mail: m-hirshb@anika.nimr.mrc.ac.uk.

§ Division of Protein Structure, National Institute for Medical Research.

|| Current address: European Bioinformatics Institute, Hinxton, Cambridge CB10 1SD, UK

⊥ Division of Physical Biochemistry, National Institute for Medical Research.

[1] Abbreviations: PBP, phosphate binding protein; MDCC, *N*-[2-(1-maleimidyl)ethyl]-7-(diethylamino)coumarin-3-carboxamide; MDCC−PBP, A197C mutant of PBP labeled with MDCC at the cysteine; IDCC, *N*-[2-(iodoacetamido)ethyl]-7-(diethylamino)coumarin-3-carboxamide.

S0006-2960(98)00428-0 CCC: $15.00
Published on Web 07/01/1998

Table 1: Data Collection and Processing Statistics

	A197C PBP·P_i	MDCC−PBP·P_i
area detector	R axis-II (in-house)	MAR (SRS station 9.5, Daresbury, U.K.)
wavelength (Å)	1.5418	0.80
temperature (K)	277	102
no. of molecules in asu	1	1
space group	$P2_12_12_1$	$P2_12_12_1$
cell dimensions		
a (Å)	42.02	41.49
b (Å)	64.16	62.65
c (Å)	124.35	122.60
resolution (Å)	25.4−2.4	12.0−1.60
no. of collected reflections	70 788	345 731
no. of unique reflections	10 913	40 945
completeness of data (%)	86.6 [69.2][a]	95.5 [93.4][a]
multiplicity	2.9 [2.1][a]	3.3 [2.9][a]
intensities $\langle I/\sigma \rangle$	9.8 [4.2][a]	11.6 [3.8][a]
R_{merge}[b]	4.7 [19.0][a]	8.0 [21.0][a]

[a] In square brackets are quantities calculated in the highest-resolution bin. [b] $R_{merge} = 100\sum|I - \langle I\rangle|/\sum I$, where I is the observed intensity and $\langle I\rangle$ is the average intensity calculated from multiple observations of symmetry-related reflections.

PBP, we have modeled the structure of P_i-free MDCC−PBP to predict the relative conformation of the fluorophore with respect to the overall structure of P_i-free PBP.

Small changes to the MDCC fluorophore on the coumarin ring, the linker, or the succinimide ring greatly reduce or eliminate the fluorescence change on binding P_i (*3*, *4*, *10*). We make use of this information to identify the features of MDCC that are important for its fluorescence properties when it is bound to PBP. The combination of structural, kinetic, and spectroscopic analysis has allowed a detailed interpretation of the interactions between the fluorophore and the protein that may facilitate the design of better probes, using this protein or other types of ligand binding proteins in combination with environmentally sensitive fluorophores.

MATERIALS AND METHODS

Crystallization. The cloning, expression, and purification of recombinant *E. coli* A197C PBP and MDCC−PBP were described by Brune et al. (*3*, *4*). A197C PBP and MDCC−PBP at 10−15 mg mL^{-1} in 10 mM Tris·HCl buffer at pH 7.6 were crystallized using the hanging-drop method (*11*). Equal volumes (1−2 μL) of protein and reservoir solutions were mixed, and the resulting drops were equilibrated against a reservoir solution containing 20−24% (w/v) PEG 6000, 20 mM potassium acetate (pH 4.5), 2 mM KH_2PO_4, and 50 mM potassium chloride. Crystals of A197C PBP and yellow crystals of MDCC−PBP appeared in 2−5 days after microseeding (*12*) at 18 and 4 °C, respectively.

Structure Determination. A197C PBP data were collected at 4 °C on a Rigaku RU200 rotating anode source equipped with mirror focusing optics. MDCC−PBP crystals were flash-frozen at 102 K using the reservoir solution and 25% (v/v) PEG 400, and data were collected on a synchrotron source (SRS station 9.5, Daresbury, U.K.). Diffraction data were processed using the package MOSFLM (*13*) and reduced using SCALA (*14*) and the CCP4 program suite (*15*). A summary of data processing statistics is given in Table 1.

The initial phases of A197C PBP were generated from the wild type structure (PDB entry 2ABH), excluding water molecules and the side chain of residue 197. The structure was built and refined through alternating cycles of O (*16*) and PROLSQ (*15*). A final refinement was carried out using REFMAC (*17*). The initial phases of MDCC−PBP were calculated from the refined A197C PBP structure. The structure including water molecules but excluding the MDCC fluorophore was built and refined using the software packages O (*16*), ARP (*18*), and REFMAC (*17*). An MDCC−thiol adduct model was generated using appropriate fragments extracted from the Cambridge Structural Database (*19*) and fitted together using the software SPARTAN (v.4, Wavefun) to obtain an energy-minimized conformation of the free MDCC−thiol adduct. The protein with the bound MDCC was then refined using REFMAC (*17*).

Table 2: Refinement Statistics

	A197C PBP·P_i	MDCC−PBP·P_i
resolution (Å)	12.0−2.4	12.0−1.6
R_{crystl} (%)[a]	17.3	17.4
R_{free} (%)[b]	22.7	20.1
rms bond length (Å)	0.015	0.009
rms bond angle (deg)	3.204	1.859
average *B*-values (Å^2)	20.2	14.9

[a] $R_{crystl} = 100\sum_{hkl}|F_o - F_c|/\sum_{hkl}|F_o|$ where F_o and F_c are observed and calculated structure factor amplitudes, respectively. [b] R_{free} is an R_{crystl} which was calculated using 5% of the data, chosen randomly, and omitted from subsequent molecular replacement search and structure refinement (*26*).

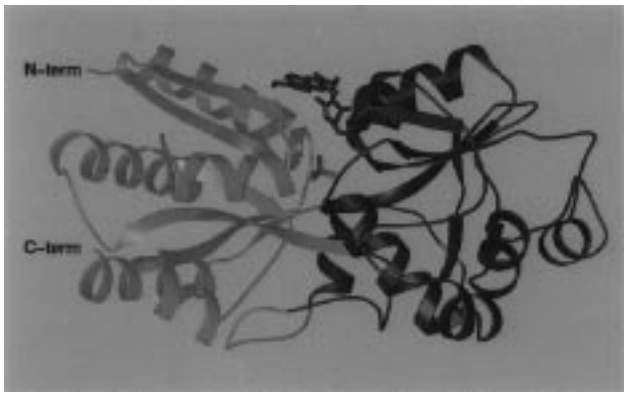

FIGURE 2: Ribbon representation of MDCC−PBP·P_i, showing the N- and C-domains, the P_i in the domain interface, and the location of MDCC. The N-domain (residues 1−77, 230−239, and 254−321) and the C-domain (residues 78−229 and 240−253) are shown in light and dark olive green, respectively. The Cys197 side chain, MDCC, and P_i are shown in stick representation and are colored red and cyan for Cys197-MDCC and P_i, respectively. This figure and Figure 3 were generated using the program BOBSCRIPT (*27*).

The refined A197C PBP and MDCC−PBP structures consist of 321 residues each and P_i with 289 and 344 water molecules, respectively. Refinement statistics are given in Table 2.

RESULTS

Overall Structure of A197C PBP and MDCC−PBP. PBP is a two-domain protein with the P_i situated at the domain interface (Figure 2). The domains share a similar three-layer $\alpha\beta\alpha$ sandwich fold, and neither domain is made up of a single continuous polypeptide segment. The N- and the C-domains, as defined by the hierarchical domain classification, CATH (*20*), belong to the lactoferrin (PDB entry 1LCF) (*21*) and the D-maltodextrin-binding protein (PDB entry 1DMB) (*22*) superfamilies, respectively.

Mutagenesis of Ala to Cys at residue 197 (A197C PBP) and MDCC labeling of Cys197 (MDCC−PBP) resulted in structures that were virtually identical to wild type PBP (PDB entry 2ABH) (*9*, *23*). The rms deviation on all main chain atoms is 0.29 Å between wild type PBP and A197C PBP, 0.24 Å between wild type PBP and MDCC−PBP, and 0.15 Å between A197C PBP and MDCC−PBP. Changes in side chain conformations of MDCC−PBP when it is compared with the wild type protein are mainly confined to accessible side chains on the protein surface. The one exception is that the position occupied by the Gln201 side chain in the wild type protein is taken by the succinimide ring in the MDCC−PBP structure, resulting in disorder of this side chain. The P_i binding site is not perturbed by either the mutation or the labeling. As in wild type PBP, P_i is monobasic and makes 12 hydrogen bonds with the protein.

MDCC Structure. The reaction of a cysteine with MDCC creates a new chiral center on the succinimide ring, resulting in two diastereoisomers (*4*). The two diastereoisomers of MDCC−PBP could not be separated, and the protein sample used in crystallization contains a 1:1 mixture of the two species. It was confirmed that the crystals themselves had equal proportions of the two diastereoisomers: crystals were isolated from the crystallization drop, washed and redissolved in buffer, and analyzed by HPLC of the tryptic digest (*4*).

In the crystal structure of MDCC−PBP, the Cys197 side chain exists in two conformations, each linked to a different configurational isomer of the MDCC−thiol adduct. This is illustrated in panels a and b of Figure 3, which show the position of the succinimide ring of each isomer. The X-ray structure of PBP−MDCC is consistent with the two isomers existing in a 1:1 ratio and were refined with 0.5 occupancy each. While the electron density of the two succinimide rings and C6 of the ethylene linker of both the *S*- and the *R*-isomers is well-defined, only one coumarin ring was observed (Figure 3c). The ethylene linker from this coumarin to the *R*-isomer succinimide is easily modeled, although density for the linker is weak and broken. The orientation of the succinimide ring of the *S*-isomer positions its C6 atom 3.1 Å from the *R*-isomer's C6. This, together with the shape of the electron density in the vicinity of the succinimide rings and considerations of acceptable bond lengths, bond angles, and torsion angles, makes it impossible for the *S*-isomer coumarin to overlap with that of the *R*-isomer. Thus, for the *S*-isomer, only the succinimide ring and C6 are traceable and no density was observed for the rest of its ethylene linker and the coumarin ring. We will return to this point in the Discussion.

The overall structure of the bound MDCC−thiol adduct and its interaction with the protein are shown in panels d and e of Figure 3. The CH_2-CH_2-NH linker connecting the succinimide and the coumarin ring of the *R*-isomer is bent so that the two rings make an angle of ∼60° with each other. The average *B*-value of the coumarin is 15 Å^2 higher than that of the whole structure, suggesting that the coumarin is more mobile than the bulk of the protein. The succinimides of both diastereoisomers have few interactions with the protein, namely, hydrophobic stabilization by the Leu291 side chain and a short hydrogen bond between the Asp292 side chain and carbonyl O3 of the *S*-isomer. The hydrophobic part of the Lys200 side chain is well-defined in the electron density map and lies about 4 Å from C6 of the *S*-isomer (Figure 3e). The position of Lys200 limits the possible positions of the disordered coumarin ring of the *S*-isomer. The coumarin ring of the *R*-isomer lies in a mostly hydrophobic groove on the face of the molecule (Figure 4). The aromatic side chain of Tyr198 is on one side of and makes an angle of ∼70° with the coumarin ring. Both Cys197 and Tyr198 belong to the C-domain. On the opposite side, the coumarin is stabilized by residues from

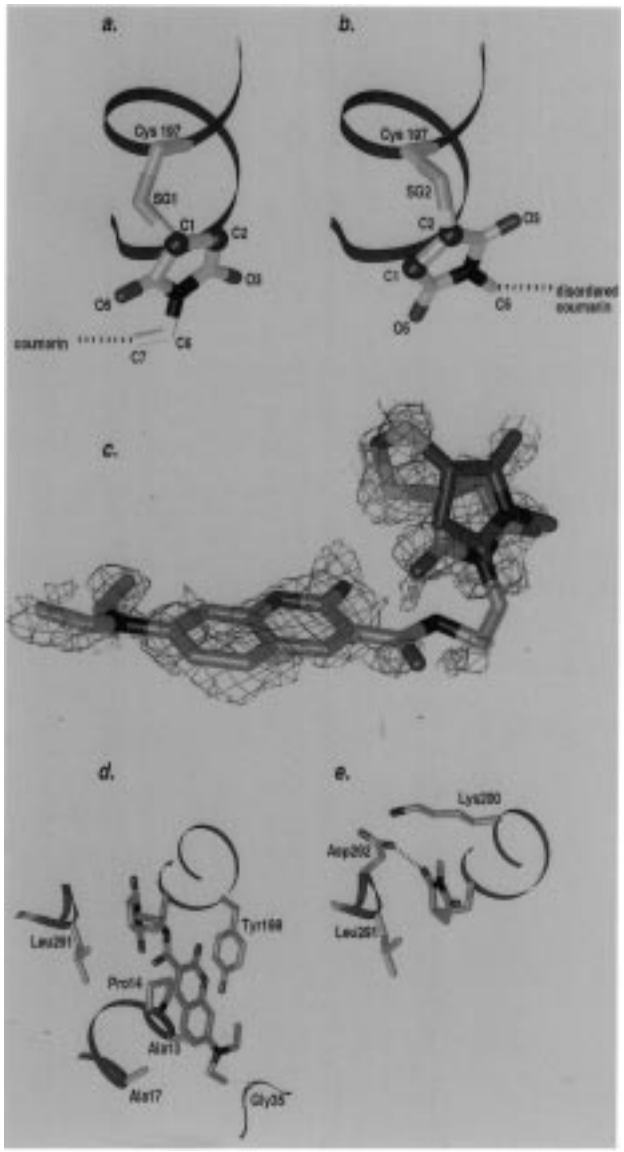

FIGURE 3: Structure of the two MDCC diastereoisomers and their interactions with PBP. (a) *R*- and (b) *S*-isomer of the succinimide rings attached to the sulfur of Cys197. The two isomers are shown in stick representation with atoms colored by atom type: oxygen, red; nitrogen, blue; sulfur, yellow; and carbon, gray. C1 and C2 of the succinimide ring are highlighted by dark green spheres. (c) A $2F_o - F_c$ omit electron density map showing the density around the MDCC−Cys adduct. The fluorophore and the side chain of Cys197 are shown by stick representation, colored by atom type with carbons of the *R*-isomer in light green and of the *S*-isomer in gray. One carbonyl of the *S*-isomer is not fully visible as its position coincides with the N−C6 bond of the *R*-isomer. The map is contoured at 1.0σ. (d) *R*- and (e) *S*-isomer binding sites. The linker and the coumarin ring of the *S*-isomer were not observed in the crystal structure. Protein residues Lys200, Tyr198, and Asp292 belong to the C-domain, while Leu291, Ala13, Pro14, Ala17, and Gly35 belong to the N-domain. Atoms are colored by atom type with carbons of Cys197-MDCC in light green and carbons of PBP in gray. The dotted line represents a hydrogen bond.

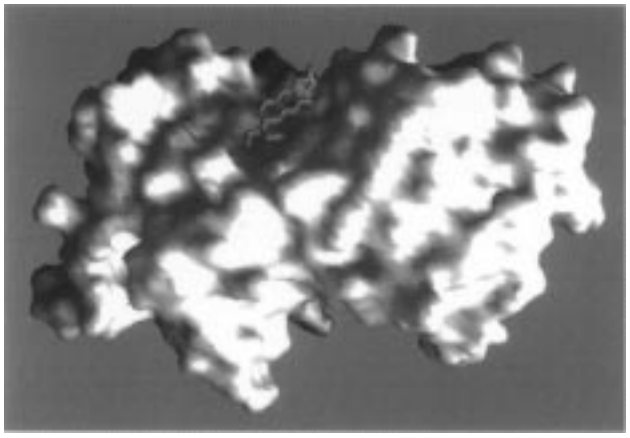

FIGURE 4: PBP molecular surface shows MDCC in the hydrophobic groove on the face of the molecule. MDCC is shown as a red stick model, and the hydrophobic groove is shaded in green. The figure was generated using the program GRASP (*28*).

the N-domain: Ala13, Pro14, and Ala17. The diethylamino substituent on the coumarin ring has several hydrophobic interactions with Ala13 and Gly35 (N-domain residues) and is coplanar with respect to the coumarin.

DISCUSSION

Overall Structure of MDCC−PBP. The coumarin moiety of MDCC−PBP lies on the surface of PBP above the P_i binding site, in a groove that is mainly hydrophobic and made up of residues from both the N- and C-domains (Figures 3d,e and 4). A striking feature of the MDCC−PBP structure is its similarity to wild type PBP, in particular, at the MDCC binding site, which shows no major readjustment of either main chain or side chain atoms of residues responsible for anchoring the coumarin. In the succinimide vicinity, Gln201 is disordered as its location in wild type PBP is taken by the succinimide ring of MDCC−PBP. The fact that the labeling of PBP was achieved without disrupting either its overall fold or the P_i binding site, consistent with the observation that P_i binding to wild type protein and P_i binding to MDCC−PBP are very similar (*4*).

The structure is consistent with there being similar amounts of the two diastereoisomers formed during the labeling reaction (*4*). There are two distinct structures for the cysteine sulfur−succinimide adduct, but only one coumarin was observed in the electron density map. We assume that the well-defined *R*-isomer of MDCC−PBP is the principal contributor to the fluorescence enhancement on binding P_i.

A second position for the coumarin that could be occupied by the *S*-isomer was not observed in the crystal structure. Stereochemical constraints imply that the unobserved coumarin of the *S*-isomer cannot be coincidental with the coumarin of the *R*-isomer. It is likely that in the crystal structure the coumarin of the *S*-isomer is intrinsically more mobile as there are no obvious hydrophobic or aromatic amino acids with which it could interact. The fluorescence data for the 1:1 mixture of isomers cannot be resolved sufficiently to give the exact contributions of each (*4*), although it is likely that the *S*-isomer has a considerably smaller fluorescence enhancement than the *R*-isomer, but not zero change, on binding P_i. The properties of the *R*-isomer therefore dominate measurements such as time-resolved fluorescence. Consequently, relate the spectroscopic properties to the structure in these terms, and in the absence of other crystal forms, solution structure (NMR), or methods of separating the diastereoisomers, we will not comment further on the *S*-isomer.

Two aspects of the fluorescent probe can be addressed by analysis of the structure of MDCC−PBP in conjunction with the solution studies (*4*). First, what features are responsible for the high-fluorescence state of the coumarin in the P_i-bound protein? Second, what structural components cause the large difference between MDCC and similar fluorescent coumarin labels in achieving this high fluorescence: i.e., what makes the interactions so specific?

Changes on Release of P_i. The P_i-free structure of PBP, determined for the T141D mutant, exhibits an opened overall quaternary fold with the two domains separated by a wide cleft (*1*). The conformational changes that PBP undergoes upon ligand binding are characterized by a hinge-bending motion of the two domains by ~25°. To predict the changes in the environment of the fluorophore on release of P_i, we assume that P_i-free MDCC−PBP adopts an overall structure similar to that of the P_i-free T141D mutant with the cleft remaining open. Therefore, we propose that, in the P_i-free MDCC−PBP, the coumarin attached to the C-domain is deprived of stabilization from contact with N-domain residues, and is left with only C-domain residue interactions, Tyr198 with the coumarin ring and Asp292 with the succinimide ring.

It is difficult to predict directly from structural considerations whether the coumarin in the P_i-free MDCC−PBP structure remains in approximately the same location with the apparent reduced stabilization from the protein. There may be mutual readjustment of the coumarin and residues in the C-domain, or the fluorophore may become mainly mobile and extended into the surrounding solvent. The 13-fold fluorescence decrease together with quantum yield and lifetime changes observed upon loss of P_i from MDCC−PBP·P_i (*4*) is consistent with a reduction in hydrophobicity in the immediate environment surrounding the chromophore.

Other spectroscopic data of Brune et al. (*4*) can be considered in terms of potential changes in interactions. First, the polarization data suggest an increased local mobility at the coumarin in the absence of P_i, along with some increase in global mobility. At least qualitatively, this is consistent with the proposed structural changes. In the P_i-free form, removal of the N-domain interactions increases the local mobility, while the remaining interactions between coumarin and protein could restrain the fluorophore from a completely free rotation relative to the protein.

The CD data can also be interpreted in terms of the proposed structural changes. The main change in the CD spectra of MDCC−PBP on binding P_i suggests a considerable increase in the asymmetric environment of the coumarin. In the presence of P_i, an asymmetric environment is evident from the structure and the fluorescence polarization data suggest a lack of mobility of the coumarin. Although the interaction with Tyr198 probably remains intact in the absence of P_i, the reduced contact of MDCC with the protein may allow the coumarin to "flip" rapidly, so effectively negating the protein asymmetry.

Role of the Diethylamino Group. Part of the hydrophobic environment of the coumarin in the MDCC−PBP·P_i complex consists of N-domain residues Gly35 and Ala13 that interact

with the diethylamino substituent on the coumarin ring. This substituent is partially disordered in the electron density map, reflecting two or more conformations that differ in rotation around the single bonds between the nitrogen and its ethyl substituents. The contribution of these interactions to the overall fluorescence of MDCC−PBP may be significant, as it has been shown that replacement of the diethylamino substituent with dimethylamino considerably reduces the sensitivity of the fluorescence signal to P_i binding. In the latter case, fluorescence increases only 60% on P_i binding (M. Brune and M. R. Webb, unpublished result).

The diethylamino group cannot rotate freely in the P_i-bound form, and the bonds to the nitrogen may remain coplanar with respect to the coumarin, allowing the nitrogen lone pair to interact with the aromatic system of the coumarin ring. It is likely that, in the P_i-free form with the cleft open, the diethylamino moiety of the coumarin can rotate freely. Coumarins in which the lone pair of the amino substituent is constrained to optimal overlap with the aromatic π-electrons are known to have high fluorescence quantum yields. Examples are Coumarin 314 (*24*) and BACM [*N*-(6-butterflyaminocoumarin-3-yl)maleimide] (*25*), where the ring structure at the amine prevents rotation. The constraints imposed by the protein on the diethylamino group in MDCC−PBP•P_i are the specific hydrophobic interactions that are likely to cause the large fluorescence enhancement.

Role of the Linker. The size of the P_i-dependent fluorescence change is very dependent on the structure of the linker between Cys197 and the coumarin (*3*). Altering the linker from ethylene to propylene or phenylene makes the coumarin less sensitive to P_i binding. These changes can be interpreted in terms of the overall structure of the MDCC fluorophore, which is bent at the ethylene linker (Figure 3c). This bend is essential in allowing the coumarin ring to occupy the hydrophobic groove on the surface of PBP. It is therefore possible to see why the fluorescence state of the coumarin is so strongly affected by the nature of the linker. Not only the length of the linker but also its flexibility are important for the precise position of the coumarin.

Using IDCC, the iodoacetamide analogue of MDCC, the fluorescence of the resulting labeled protein is also much less sensitive to P_i (*4*), an observation that cannot be explained by the required bend in the linker. This molecule when bound to PBP has the same number of bonds between the sulfur and coumarin as in MDCC−PBP and enough torsional degrees of freedom to allow the placement of its coumarin ring to be the same as that in MDCC−PBP. A possible explanation for the reduced sensitivity of IDCC is that binding of its coumarin is insufficient to overcome the extra entropy of the more flexible chain. The relatively rigid succinimide ring of MDCC−PBP has fewer degrees of freedom.

In conclusion, the MDCC−PBP crystal structure provides a detailed view of the interactions of fluorophore with PBP and the features responsible for its high-fluorescence state in the presence of P_i. The detailed characterization (*4*) has enabled us to obtain considerable insight into how the interaction with protein residues produces the observed spectroscopic properties. This combination of studies has rarely been possible, and we expect it to be useful in the general understanding of proteins labeled with environmentally sensitive fluorophores.

ACKNOWLEDGMENT

We thank Dr. Hartmut Luecke (University of California, Irvine, CA) for assistance during the early stages of the project, clarifying several aspects of the crystallization of wild type PBP, and providing us with the coordinates of wild type PBP. We also thank Dr. Liz Carpenter (National Institute for Medical Research) for helping in data collection.

REFERENCES

1. Ledvina, P. S., Yao, N. H., Choudhary, A., and Quiocho, F. A. (1996) *Proc. Natl. Acad. Sci. U.S.A. 93*, 6786−6791.
2. Quiocho, F. A. (1991) *Curr. Opin. Struct. Biol. 1*, 922−933.
3. Brune, M., Hunter, J. L., Corrie, J. E. T., and Webb, M. R. (1994) *Biochemistry 33*, 8262−8271.
4. Brune, M., Hunter, J. L., Howell, S. A., Martin, S. R., Hazlett, T. L., Corrie, J. E. T., and Webb, M. R. (1998) *Biochemistry 37*, 10370−10380.
5. Gilbert, S. P., Webb, M. R., Brune, M., and Johnson, K. A. (1995) *Nature 373*, 671−676.
6. Nixon, A. E., Brune, M., Lowe, P. N., and Webb, M. R. (1995) *Biochemistry 34*, 15592−15598.
7. Lionne, C., Brune, M., Webb, M. R., Travers, F., and Barman, T. (1995) *FEBS Lett. 364*, 59−62.
8. He, Z. H., Chillingworth, R. K., Brune, M., Corrie, J. E. T., Trentham, D. R., Webb, M. R., and Ferenczi, M. A. (1997) *J. Physiol. 501*, 125−148.
9. Luecke, H., and Quiocho, F. A. (1990) *Nature 347*, 402−406.
10. Corrie, J. E. T. (1994) *J. Chem. Soc., Perkin Trans. 1*, 2975−2981.
11. McPherson, A. (1982) *Preparation and Analysis of Protein Crystals*, Wiley, New York.
12. Stura, E. A., and Wilson, I. A. (1990) *Methods−A Companion to Methods in Enzymology*, Vol. 1, pp 38−49, Academic Press, San Diego.
13. Leslie, A. G. W. (1992) *CCP4 and ESF-EACMB Newsletter on Protein Crystallography*, p 26, Daresbury Laboratory, Daresbury, U.K.
14. Evans, P. R. (1993) *Proceedings of CCP4 Study Weekend on Data Collection and Processing*, pp 114−122, Daresbury Laboratory, Daresbury, U.K.
15. CCP4 Collaborative Computational Project Number 4 (1994) The CCP4 suite: Programs for Protein Crystallography, *Acta Crystallogr. D50*, 760−763.
16. Jones, T. A., Zou, J. Y., Cowan, S. W., and Kjeldgaard, M. (1991) *Acta Crystallogr. A47*, 110−119.
17. Murshudov, G. N., Vagin, A. A., and Dodson, E. J. (1997) *Acta Crystallogr. D53*, 240−255.
18. Lamzin, V. S., and Wilson, K. S. (1993) *Acta Crystallogr. D49*, 129−147.
19. Allen, F. H., and Kennard, O. (1993) *Chemical Design Automation News 8*, 31−37.
20. Orengo, C. A., Michie, A. D., Jones, S., Jones, D. T., Swindells, M. B., and Thornton, J. M. (1997) *Structure 5*, 1093−1108.
21. Smith, C. A., Anderson, B. F., Baker, H. M., and Baker, E. N. (1994) *Acta Crystallogr. D50*, 302−316.
22. Sharff, A. J., Rodseth, L. E., and Quiocho, F. A. (1993) *Biochemistry 32*, 10553−10559.
23. Yao, N., Ledvina, P. S., Choudhary, A., and Quiocho, F. A. (1996) *Biochemistry 35*, 2079−2085.
24. Fletcher, A. N., and Bliss, D. E. (1978) *Appl. Phys. 16*, 289−295.
25. Chaurasia, C. S., and Kauffman, J. M. (1990) *J. Heterocycl. Chem. 27*, 727−733.
26. Brünger, A. T. (1992) *Nature 355*, 472−475.
27. Esnouf, R. M. (1997) *J. Mol. Graphics 15*, 133−138.
28. Nicholls, A., Sharp, K. A., and Honig B. (1991) *Proteins: Struct., Funct., Genet. 11*, 281−296.

BI980428Z